IMAGE PROCESSING FOR BIOLOGICAL EXPERIMENTS ON A MOBILE PHONE

BY

HUY MINH LE

THESIS

Submitted in partial fulfillment of the requirements
for the degree of Master of Science in Electrical and Computer Engineering
in the Graduate College of the
University of Illinois at Urbana-Champaign, 2016

Urbana, Illinois

Adviser:

Associate Professor Steven Sam Lumetta

Abstract

Smartphone capabilities have been expanding rapidly since Apple Inc. introduced the iPhone in early 2007. Today's smartphones offer decent computational power, good internet connectivity and high-pixel-count cameras. In this thesis, we leverage these resources in novel ways, using a smartphone CMOS camera as a sensing device and performing biological analyses immediately on the smartphone. We show two novel ways to exploit the capacities of the smartphone and discuss the challenges that we faced in the development of these applications.

We first demonstrate a mobile system to identify counterfeit and substandard drug products effectively and inexpensively. Our system costs roughly $250, which is affordable in developing countries in Africa and Asia, where counterfeit and substandard drug products are flooding the markets. The system also enables analyses at the point of testing, which is particularly valuable when laboratory facilities are remote or unavailable. The system consists of a 3D-printed cradle, a cheap Android based smartphone and an UV lamp. The system is inspired by the use of the thin layer chromatography (TLC) method, which is known to be efficient in verifying the identity of drug products from unknown sources. The core analysis of a TLC plate is performed though a series of image processing algorithms on the Android smartphone. For drugs with a single active pharmaceutical ingredient (API) that absorbs ultraviolet (UV) light, the mobile phone-based detection system is able to discern 5% drug concentration differences, which is equivalent to a commercially available lab-based desktop TLC reader priced at roughly $40,000.

We then demonstrate absorption-based biological assays by performing an enzyme-linked immunosorbent assay (ELISA) experiment. ELISA is an assay technique used to detect and quantify substances such as proteins, antibodies, hormones, etc. When combined with some simple optical components, the rear-facing CMOS camera in a smartphone can capture spectral data for biological samples. We developed image processing algorithms to calibrate and to analyze these spectra to match the results produced by conventional laboratory instruments. In order to enable unskilled users to perform ELISA experiment accurately, we integrated these techniques into an Android application with a simple user interface that walks users though assay steps.

Finally, we generalize some of the lessons learned and challenges faced during development of the TLC and ELISA applications in order to provide a broader and more useful picture for developing smartphone bioassay applications in general.

Acknowledgments

I would first like to thank my thesis advisor, Associate Professor Steven Sam Lumetta of the Electrical and Computer Engineering Department at the University of Illinois at Urbana-Champaign. The door to Prof. Lumetta's office was always open whenever I ran into trouble or had a question about my research or writing. He consistently allowed this paper to be my own work, but steered me in the right the direction whenever he thought I needed it.

Contents

1. Introduction 1
1.1 Identification of counterfeit and substandard drug products 1
1.2 Absorption-based biological assays 2
2. Background 4
2.1 Drug identification using thin layer chromatography 4
2.2 Enzyme linked immunosorbent assays (ELISA) 5
3. Thin layer chromatography context 7
3.1 Preparation of sample stock and working solutions 7
3.2 Chromatography and densitometric scanning 8
3.3 Smartphone thin layer chromatography analyzer 8
4. TLC image analysis algorithms 10
4.1 Pre-processing 10
4.2 Origin and solvent front detection 10
4.3 Spot detection 12
4.4 Absorption measurement 14
4.5 Multi-spot processing 16
5. Absorption-based biological assays 17
5.1 Hardware design 17
5.2 Software design 18
5.2.1 Pre-processing 19
5.2.2 Laser calibration 19
5.2.3 Spectrum processing 20
5.2.4 Absorption measurement 21
5.2.5 Four parameter logistic regression 21
6. Lessons learned and challenges 22
6.1 Unstable and uneven illumination 22
6.1.1 Unstable illumination 22
6.1.2 Uneven illumination 26
6.2 Thin layer chromatography modeling 26

6.3 Camera characteristics 27
6.4 Optimization for smartphone computation 29
6.4.1 Optimization using single instruction multiple data (SIMD) instructions 29
6.4.2 Filter consideration 29
6.5 Hardware design 29
7. Conclusion 31
References 32

1. Introduction

In early 2007, Apple Inc. introduced the iPhone, one of the first smartphones having a multi-touch interface. The IPhone debut was a great success and drove the industry toward the smartphone generation. Since then, the capabilities of smartphones have quickly expanded. Today, we can buy a smartphone with decent computational power, good internet connectivity and high-pixel-count cameras with a few hundred dollars. Inspired by the rapid advance in smartphone technology, many applications have been developed to fulfill humanity's needs in areas such as social networks, messaging, web searching, online dating, etc. In this thesis, we explore the possibility of leveraging smartphone capabilities in an unprecedented way by utilizing a smartphone for performing biological experiments. Traditionally, a typical biological equipment needs a high-end camera to capture biological image data and a desktop computer to process the data. Since we have a decent computational power and good cameras on a smartphone, with appropriate extensions, we can turn a smartphone CMOS camera into a sensing device and perform biological analyses directly on the smartphone. Towards that end, we demonstrate two novel ways to exploit the capacities of the smartphone: identification of counterfeit and substandard drug products and absorption-based biological assays.

1.1 Identification of counterfeit and substandard drug products

Counterfeit and substandard drug trade, a multibillion dollar industry, is thriving in the markets of many developing countries. According to the World Health Organization, counterfeit and substandard drugs account for up to 30% of sales of pharmaceuticals in many developing countries of Africa and parts of Asia [1]. These products pose severe health risks for patients who receive doses that are lower than those that are required for effectiveness, or receive doses that have no therapeutic indication for the disease of concern. The most common incidences of falsified critical drugs are encountered in the treatment of malaria, HIV/AIDS, tuberculosis, and cancer, thus these products pose an extreme health risk to the patients who take them. An estimated 100,000 deaths per year have been linked to the fake drug trade in Africa [2]. Thus, there is an urgent demand for an efficient and low-cost technology for identification of these products in the drug supply chain. Furthermore, such a detection system can be combined with an information-sharing network that will enable such products to be rapidly identified and marked by their source, batch number, packaging and physical appearance.

Thin layer chromatography (TLC), originally introduced in the 1950s to separate compounds, is also known to be effective in verifying the identity of drug compounds, especially of suspicious drug compounds from unknown sources. TLC is performed on a TLC plate which is a sheet of glass, plastic or

aluminum foil, coated with an absorbent layer. After developing TLC plates, we need to send them into a TLC reader to perform image capturing and then image analysis. Commercial TLC readers incorporating flatbed scanners or CCD cameras, white light illumination or high intensity UV lamps interfacing with a personal computer have been developed and widely adopted, with prices in the range of US $5000 - 45000. These prices are inaccessible to labs in developing countries in Africa and Asia.

In this work, we present a mobile TLC reader comprising a 3D-printed plastic cradle, a Samsung Galaxy Fame smartphone and a battery-powered UV lamp together with a series of efficient image processing algorithms to realize the goal of smartphone TLC. The system is compact, light-weight (700 g, including the smartphone and the UV lamp with four 1.5 V AA batteries), and inexpensive (3D-printed cradle: US $130, handheld UV lamp: US $63, smartphone: US $59.99). While we chose to use an inexpensive smartphone for affordability in developing countries, the approach demonstrated can be easily adjusted to any mobile device with decent computational power and high pixel count rear-facing camera. In addition to the detection hardware, we developed an Android application with a series of image processing algorithms to identify the location and intensity of spots. Spots appear at positions related to the specific molecular composition of drugs present in the samples, and the intensities of the spots are related to the concentrations of those drugs. These two together enable our system to estimate both the type and the concentration of a drug in an unknown sample. We compared our system directly to measurements taken with a commercially available densitometer (TLC Scanner 3; CAMAG, Muttenz, Switzerland) for a set of TLC plates prepared with 100%, 95%, and 75% concentrations of nevirapine (an anti-retroviral product), amodiaquine (an anti-malarial and anti-inflammatory product), and paracetamol (an anti-inflammatory product). The results show that the smartphone-based TLC system provides measurements for location and spot intensity that are equivalent to those taken with the commercial instrument [3].

1.2 Absorption-based biological assays

Using a basic spectroscopy system to detect light reflected/transmitted from a biosensor surface, a smartphone-based detection instrument can be readily extended to perform most common classes of label-based assays. In this work, we perform enzyme linked immunosorbent assay (ELISA) by measuring the optical absorption spectra of a liquid test sample as an enzyme-substrate interaction, modulated by the presence of a specific analyte that generates colored products.

The system employed in this work comprises a 3D printed cradle and a Samsung Galaxy S3 smartphone. The cradle holds several optical components aligned so as to maximize the intensity of light delivered to

the phone's CMOS camera sensors. We developed an application that runs on the smartphone to enable an unskilled user to perform assays accurately, and that provides assay results to the user. ELISA requires per-experiment standardization based on curve-fitting, which can be performed completely on the phone so as to eliminate the need for users to perform data recording and entry into a desktop application.

2. Background

2.1 Drug identification using thin layer chromatography

Originally invented to separate colored plant pigments, thin layer chromatography (TLC) evolved over time and became a method for visualization of uncolored compounds on exposure to UV radiation. Figure 1 illustrates sample preparation of a TLC system. The samples (solutes), once in solution, are applied onto a TLC plate. Usually, three samples are spotted onto a TLC plate: the lower and higher acceptable limits of the drug we wish to identify and an unknown drug sample we wish to test against. The plate itself consists of a solid support, for instance plastic, glass or aluminum, coated with an adsorbent layer (stationary phase) specially chosen for the separation and fluorescent compound. The solutes are applied to the plate along an origin line parallel to the bottom of the plate. The plate is then placed in a tank (developing chamber) containing an eluting solvent (mobile phase) which flows over the

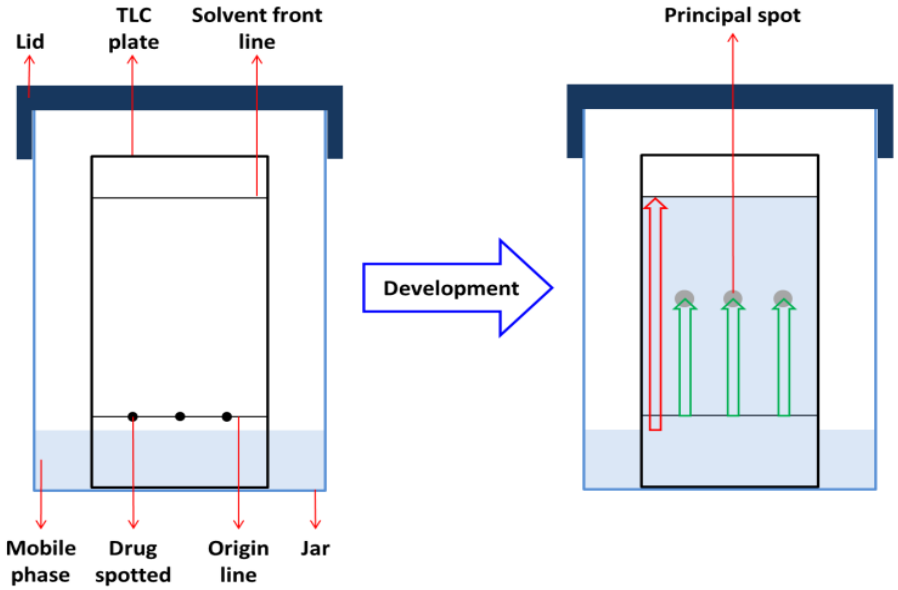

Figure 1: (replicated from [3]) Illustration of TLC plate development process. TLC utilizes a solid substrate support (most commonly a 200 µm thick strip of aluminum) that is coated with a stationary phase (silica gel, layer thickness: 200 ~ 250 µm). The stationary phase is infused with a fluorescent indicator compound (manganese activated zinc silicate) that emits a broad band of wavelengths in the green part of the visible spectrum when excited by UV light (λ = 254 nm). The substrate and stationary phase compose the TLC plate. TLC plates are mass-manufactured in standard size format, and the conventional format used in our work is 50 × 100 mm. Chromatographic separation using TLC is initiated by manually spotting aliquots of the drug sample and the references along an origin line placed 15 mm from one edge. The origin line is marked with a horizontally drawn pencil line. After the spots dry, the plates are placed into a developing solution (mobile phase) in a closed jar. The mobile phase travels vertically along the stationary phase via capillary action. As the mobile phase moves past the origin line, the drug components are drawn upwards and travel with the mobile phase through the stationary phase at different rates depending on their molecular polarities. The distance that the mobile phase front (or solvent front) should travel during the test is typically marked with a pencil-drawn line before the plate development. The TLC plate development is stopped when the mobile phase reaches this line. The plate is then removed from the jar and allowed to dry. Even though the principal spots are not visible without UV illumination, they will be located between the origin line and the solvent front line. This TLC development process takes an hour.

plate due to capillary action and drives the solute away from its origin across the plate. Before the solvent front reaches the plate's top end, the plate is removed from the tank and the solvent's finish position is marked as the front line. After development, the chromatoplate is dried off to remove all residual solvent. For UV-absorbing drugs, when the plate is illuminated with the UV light, the fluorescent compound emits green light that is reduced in intensity by the UV-absorbing drugs, resulting in dark spots on a bright green background.

Drug identity is verified by retention factor (R_f) which is defined as:

$$R_f = \frac{the\ distance\ traveled\ by\ the\ spot}{the\ distance\ traveled\ by\ the\ solvent\ front}$$

Whether an unknown sample contains the desired active ingredient can be determined by comparing the R_f of the unknown sample with the R_f of the calibration samples. For qualitative analysis, there is strong evidence that the drugs in the test and standard solution are identical if the spots of both samples show roughly the same R_f values. When the unknown sample identity is confirmed to be the same as calibration samples, the concentration of the unknown sample can be evaluated using spot intensity. By comparing the spot intensity resulting from the unknown sample to the calibration samples, the concentration of the target drug in the unknown sample can be estimated.

2.2 Enzyme linked immunosorbent assays (ELISA)

The following description of ELISA was written by Kenneth D. Long [4]:

"ELISA assays represent one of the most widely used methods for detection of a substance (typically an antigen, such as a virus or a protein) in a liquid sample. They are commonly used as medical diagnostic tests, but they have also been adopted for many other applications that include plant pathology and various forms of manufacturing quality control. Briefly, a solid surface (such as the surface of a microplate well) is prepared with an antibody that selectively captures an analyte from a test sample. After capture of the analyte, a secondary antibody (recognizing a different location on the analyte than the capture antibody) is applied to the surface. The secondary antibody is linked to an enzyme, and a substrate to that enzyme is introduced to the liquid solution, so that the enzyme-substrate interaction generates colored products. In this process, the enzyme is not consumed, so the amount of colored product accumulates the longer the interaction can occur. Based upon this basic principle, several distinct types of ELISA assays have been developed (Indirect ELISA, Sandwich ELISA, Competitive ELISA), which share the detection method of quantifying the "optical density" of the liquid sample to determine

the concentration of colored reaction products. ELISA assays are performed in a transparent container of known dimensions (a “cuvette”), by measuring the intensity of light transmission through the cuvette at specific wavelengths.

“Because ELISA can measure the presence of an antibody or antigen in a sample, it has proven to be a useful tool for determining serum antibody concentrations (such as for the HIV and hepatitis B viruses), and for detection of allergens in food. ELISA is also used in toxicology applications for detection of certain classes of drugs. A wide variety of laboratory ELISA assay readers, configured for use with microplates, are commercially available, while only a few handheld portable ELISA readers are offered for specific applications. Smartphone-based ELISA detection has not been demonstrated to our knowledge.”

3. Thin layer chromatography context

In this study, we selected drugs that are often targeted for imitation by unscrupulous drug manufactures: paracetamol, nevirapine, and amodiaquine. Paracetamol is a drug used to treat pain and fever [5]. Nevirapine is a drug used to treat and prevent HIV/AIDS, particularly HIV-1 [6]. Amodiaquine is a drug used to treat malaria [7]. Each drug is sold in tablet form and contains a single API that absorbs UV light [8]. Paracetamol was obtained from Zenufa Laboratories, Ltd. (Dar-Es-Salaam, Tanzania); nevirapine from Laboratories, Ltd. (Secunderabad, India); amodiaquine from Shelys Pharmaceutical, Ltd. (Dar-Es-Salaam, Tanzania). For other TLC preparation materials, please refer to our paper [3].

3.1 Preparation of sample stock and working solutions

The sample stock and working solutions were prepared by Dr. Eliangiringa Kaale. The following is his description:

"The procedures used for performing the TLC spotting and development are described in the Global Pharma Health Fund Minilab® manuals. One tablet (paracetamol 500 mg, amodiaquine 200 mg, or nevirapine 200 mg) was ground into a fine powder while wrapped in aluminum foil, and the powder was transferred into a 100-mL volumetric flask containing 40 mL of methanol. The flask was shaken for three minutes to dissolve the API and was set to stand for approximately five minutes to allow the undissolved residue to settle, leaving a clear supernatant liquid. Appropriate amounts of methanol were then added to the flask to obtain the target of 5 mg/ml. Aliquots were drawn from the supernatant stock sample solutions to prepare 100%, 95%, and 75% solutions (Table 1)". [3]

Table 1: Summary of sample stock and working solution concentrations

Pharmaceutical product	Stock sample solution [mg/ml]	Working sample solutions [mg/ml]		
		100%	95%	75%
Paracetamol	5.0	1.25	1.19	0.94
Amodiaquine	5.0	0.63	0.59	0.47
Nevirapine	5.0	1.25	1.19	0.94

***** The amounts of API added depended on the absorptivity of the compound; the higher the absorptivity, the lower the concentration to keep the quench at an optimum level.

3.2 Chromatography and densitometric scanning

The chromatography and densitometric scanning were performed by Dr. Thomas Layloff. The procedure he followed to perform the scanning was as follows:

"The solvent front line was pre-marked at 70 mm from the bottom of the TLC plate. Two microliters of the test solutions were manually placed on the plate along the origin line as a spot using precision 2-microliter capillaries. After spotting, the plates were air-dried and then placed into the developing jar. The developing jar was lined with filter paper on one long side to aid saturation, and the mobile phase was poured into the jar. The composition of the mobile phase for each drug is shown in Table 2. The jar lid was closed for 20 minutes to saturate the tank before the plate was developed. After the plate was placed into the jar and the mobile phase front proceeded to the pre-marked solvent front line, the plate was removed and allowed to dry for three to five minutes. After drying, the plates were scanned using the conventional densitometer (UV illumination: peak = 254 nm). The detector slit parameters were set at 6 × 0.45 mm, the scanning speed was set at 20 mm/s, and the data resolution was set at 100 m/step. The data capture and calculations obtained from the scanned plates were performed with the instrument-supplied planar chromatography manager software (winCATS 1.4.3; CAMAG)."[3]

Table 2: Mobile phase composition ratio

Pharmaceutical product	Composition ratios			
	Ethyl acetate	Toluene	Methanol	Ammonia
Paracetamol[1]	24	·	3	1
Amodiaquine[2]	10	·	40	1
Nevirapine[3]	11	4	5	·

(1) Pharmweb Web site. http://www.pharmweb.net/pwmirror/library/tlc/tlcall.pdf (accessed Dec 26, 2015).
(2) GPHF-Minilab Web site. http://www.gphf.org/images/downloads/previous_manuals/manual_2_vol4_en.pdf (accessed Dec 26, 2015).
(3) GPHF-Minilab Web site. http://www.gphf.org/images/downloads/previous_manuals/manual_2_vol3_en.pdf (accessed Dec 26, 2015).

3.3 Smartphone thin layer chromatography analyzer

Our smartphone TLC analyzer hardware as described in Fig. 2 consists of a cradle fabricated using a 3D-printer, a Samsung Fame smartphone and an UV lamp. The cradle acts as a container to hold the smartphone and the UV lamp. We chose Samsung Fame based on the balance of good camera capabilities and reasonable price. Another benefit of this smartphone is that it runs the Android operating system, which allows us to modify settings such as white balance, exposure time etc. The UV lamp is a small, handheld model that provides UV illumination centered at 254nm. To keep the UV lamp

lighting stable, we need to warm it up for about 200 seconds. The hardware was designed and fabricated by Hojeong Yu.

Figure 2(f) shows a sample TLC plate image captured by our system. From the sample TLC image, we determine the origin line, the solvent front, and then segment out spots. Next, we identify spot centers and calculate R_f values as defined in Section 2.1. Finally, if R_f values are roughly the same, we distinguish spots based on spot intensities, as described in Section 4.4.

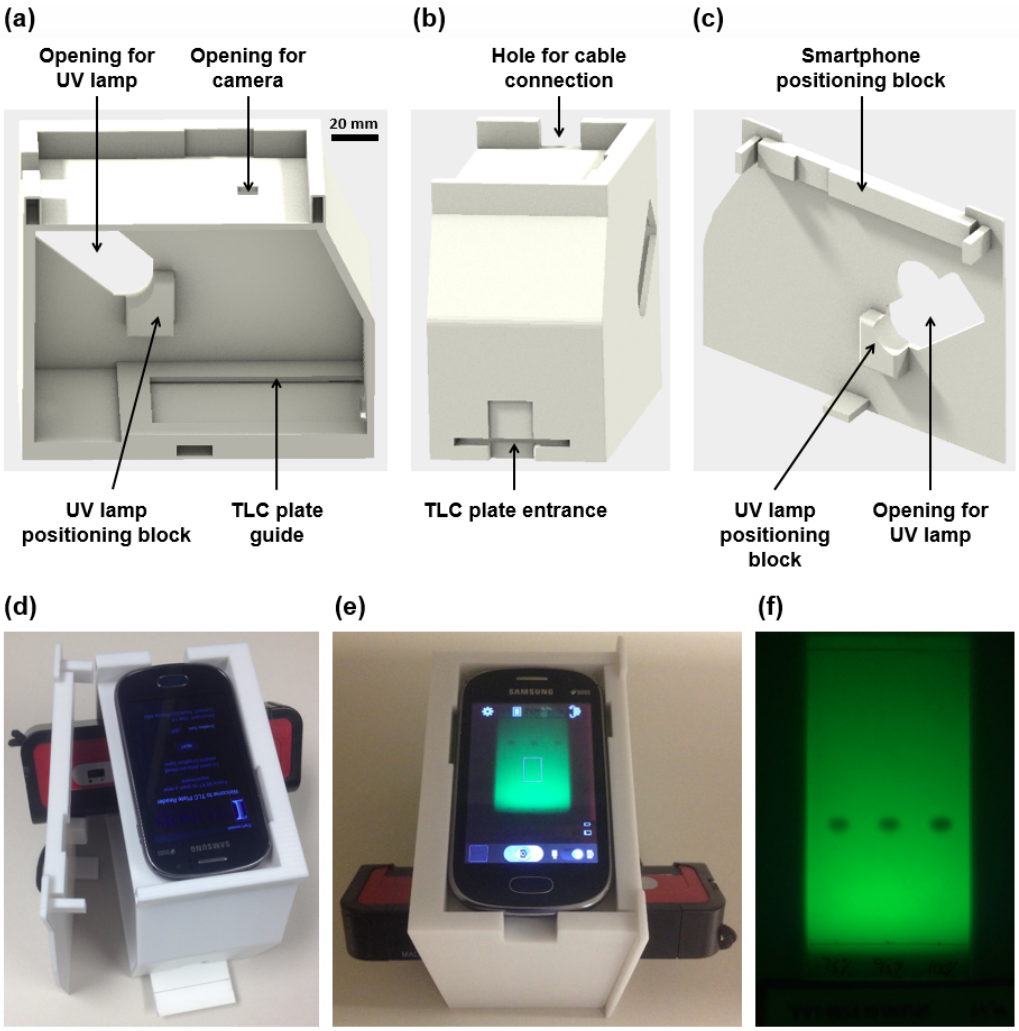

Figure 2: Illustration of the smartphone TLC analyzer and photographs of the system. (a, b) Illustration of the cradle that holds a smartphone, a UV lamp, and a TLC plate. (c) Illustration of the cover provides a dark environment and that mechanically supports the lamp. (d) Photo of the assembled smartphone TLC analyzer. (e) Photo of the TLC plate analysis (image capturing/processing). (f) Captured full image of the TLC plate.

4. TLC image analysis algorithms

This section describes image processing algorithms that we developed to perform TLC analysis on a smartphone. We start with pre-processing steps, then show how we detect the origin and the solvent front line. After that, we present our spot detection algorithm and end with how we measure UV light absorption to estimate drug concentration.

4.1 Pre-processing

An unprocessed RGB image taken by the smartphone consists of a matrix of 2560 x 1920 x 3 pixels, where pixel value is an integer in the range [0, 255]. To simplify processing, we convert pixel values to floating point numbers in the range [0, 1]. Images captured by CMOS sensors suffer from various noise sources, including shot noise, thermal noise, and readout noise, that lead to fairly high variance in individual pixel measurements if only a single image is used, as described in Chapter 6.3. To increase signal-to-noise ratio (SNR), we average 10 consecutive images to generate a single image. Thus, from this point, the TLC image refers to the averaged image. The black boundaries that appear in the TLC image are due to physical constraints in the cradle, and are fixed across images. Consequently, to make subsequent steps become easier, we remove those boundaries. Since for detecting lines and segmenting out spots, luminance matters most for us, we convert the image from RGB color space to YCrCb color space using the following formula and process on the luminance channel (Y). There is no unique way to convert from RGB to illuminance; the way we demonstrate here is based on the human perception and the conversion works for us so we just stick to the formula for now.

$$Y = 0.2989R + 0.5866G + 0.1144B$$

4.2 Origin and solvent front detection

Our detection algorithm for determining the position of the origin line and solvent front line is derived from edge detection algorithms [9] with an assumption that these lines are parallel to the top and bottom edges of the TLC plate. First, we blur the TLC image by filtering the TLC image with a 2D Gaussian filter with sigma of four. This step smooths the image and removes high-frequency noise. However, the lines that we need to detect belong to the high-frequency part of the image as well. Therefore, we face a tradeoff between blurring and localizing the edges. The tradeoff is determined by the width (sigma) of the Gaussian filter. Sigma of four works well for our dataset in terms of blurring the image without losing the localization of the edges. Also, when applying a 2D Gaussian filter, it is customary to choose a filter size of six sigma with an odd width and height for symmetry with the central peak. With sigma of four, six sigma is 24, our filter size is 25 by 25. After smoothing with the Gaussian, we filter the resulting

image with the filter $[1\ -2\ 1]^T$. This step serves the purpose of taking the second derivative of the image in the vertical direction. Since we assume that lines are parallel to the top and bottom edges of the TLC plate, we sum the result of the previous step in the horizontal direction to make the final localization step easier. To localize lines in the last step, we search for the positions of the two strongest local peaks. A local peak is defined as a data sample larger than its two neighbors. The peak near the top of the image corresponds to the solvent front, and the peak near the bottom of the image corresponds to the origin. The front line and origin line detection algorithm is summarized as Algorithm 1 and an instance of executing the algorithm is illustrated in Figure 3. After locating the origin line and the front line, we crop them from the original image and use the cropped original for the spot detection step.

Algorithm 1: Origin and Solvent Front Detection

1. Filter the TLC image by 2D Gaussian filter with sigma of four.
2. Filter the result of step 1 with filter $[1\ -2\ 1]^T$.
3. Horizontally sum the result of step 2.
4. Search for the positions of two strongest local peaks. The peak near the top of the image corresponds to the solvent front, and the peak near the bottom of the image corresponds to the origin.

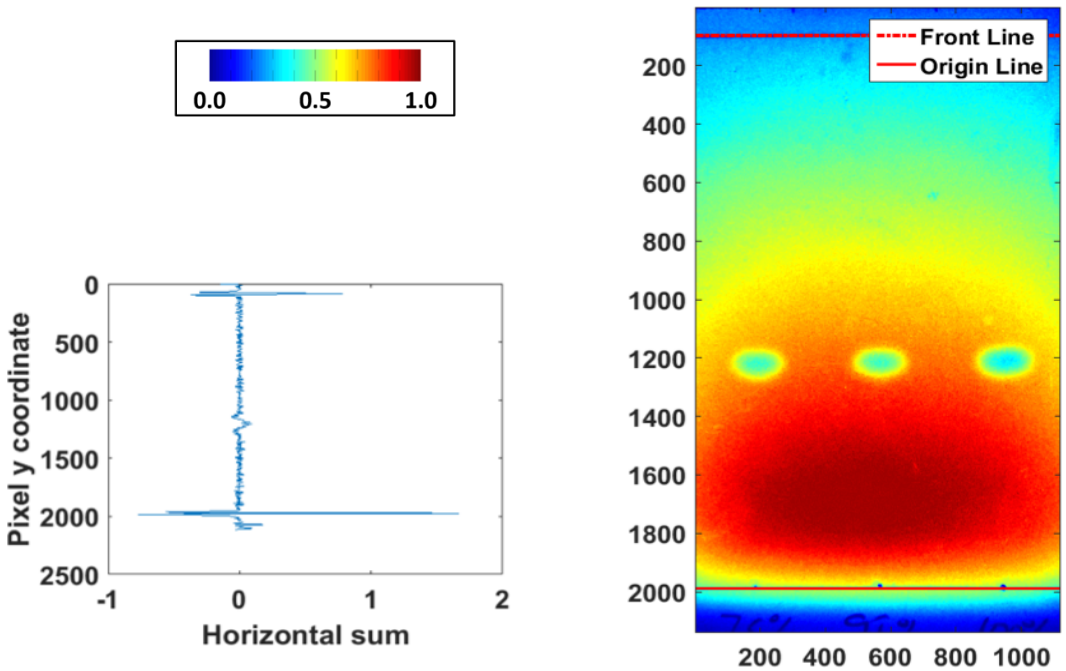

(a) (b)

Figure 3: (a) Result of horizontally summing filtered response. (b) Result of lines detection algorithm.

4.3 Spot detection

Spots are composed of the lowest intensity pixels in a TLC image. Therefore, we choose to employ global thresholding, which means using a threshold to convert an image into a binary image. Pixels with values at or above the threshold are assigned a value of 1, and pixels with values below the threshold are assigned a value of 0. Global thresholding is simple, fast, and requires little computation. However, variations in the UV illumination intensity across the plate cause problems with direct application of global thresholding. We correct for this effect by multiplying the image by the inverse of a blank plate image. Figure 4(a) illustrates the result of this normalization step. After blank plate correction, we segment out spots by setting a threshold that separates out the darkest 4% pixels. This threshold was chosen experimentally using several plates in our dataset, then shown to be effective for the remaining plates in the dataset (27 in total), and results in good visual results for spot segmentation. We further clean up noise in the binary image using a morphological image processing technique. Figure 4(b) illustrates the result of segmentation. At this stage, we have a binarized image with spots separated from the background. Spots are then located using a connected component algorithm with eight connectivity, which means that any two pixels are considered connected whenever they are adjacent in horizontal, vertical, or diagonal directions. We then extract data from the resulting components (each is a spot). To find the center of a spot, we draw a bounding box around the spot and sum the region in the normalized image (not the binary one) in both the vertical and horizontal directions. The center coordinates are located by finding the minima of fitted quadratic curves to those 1D summed signals. We could use the center of the box as the center of the spot, but spot edge effects (due to residual illumination as well as variations in motion of the drug) can be non-uniform, so fitting is a better approach. From the center position of each spot, we can derive the R_f as defined in Section 2.2. The entire algorithm is summarized as Algorithm 2. At this point, we can render a decision whether the unknown sample contains the same active ingredient as the calibration samples based on R_f values. If the R_f value of the unknown sample is significantly different from R_f values of calibration samples, the unknown sample does not contain the desired active ingredient and should be rejected. If R_f values are roughly the same, we continue by estimating UV light absorption in order to evaluate the concentration of the unknown sample.

Algorithm 2: Spot detection

1. Multiply the image by the inverse of a blank plate image to obtain the corrected illumination image.
2. Compute a histogram of image brightness and select a threshold to separate the 4% darkest pixels.
3. Use global thresholding to obtain a binary image based on the 4% threshold.
4. Apply binary opening mathematical morphological operator [10] with disk structure of radius 15, which remove small dots that are unlikely the spot of interest.
5. Locate spot regions using a connected components algorithm with eight connectivity. This step produces a mask image for each spot.
6. Using the mask for each spot in step 5, extract spot data from corrected illumination image from step 1.
7. For a spot, draw a bounding box around it, then locate the center coordinates by finding the minima of fitted second polynomial curves to the horizontal and vertical sum of the region.
8. Derive the R_f value for each spot, which is just the normalized vertical position of the spot in the photo, where 0 is the origin line and 1 is the solvent front line.

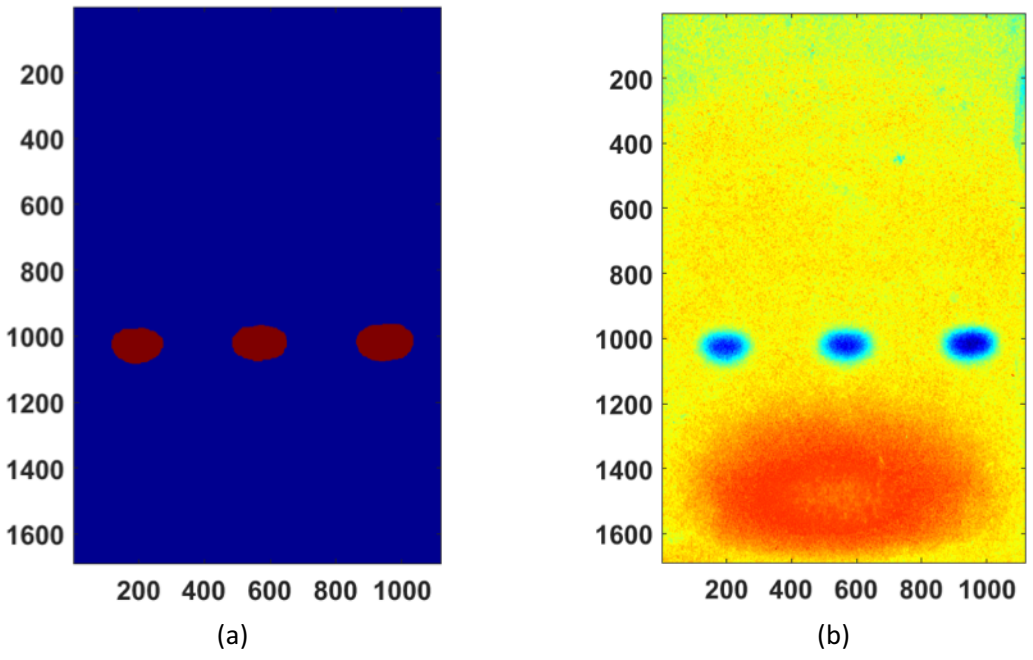

Figure 4: (a) Result of multiplying the image by the inverse of a blank plate image. (b) Result of converting (a) into a binary image by using a global threshold.

4.4 Absorption measurement

Although quantification of TLC measurements has received significant attention from the chemistry research community, none of the models that we found could be applied directly to our system. In this work, we suggest a metric to quantify absorption measurement of UV absorbing drugs. Observe that the amount of UV light absorbed depends on the amount of active ingredient present on the TLC plate, which in turn depends on the concentration of the sample. Lower concentrations absorb less UV light and produce lighter spots, while higher concentrations absorb more light and produce darker spots. Thus, to quantify absorption measurement, we integrate the absorption values of the 441 pixel intensities around the center of each spot (which is 10-pixel distance from the center of the spot each side). The number of integrated pixels was chosen empirically based on our test TLC plates. The absorption value is measured as 1-pixel intensity, where pixel intensity ranges from 0 to 1. Since the TLC image that we obtain from the camera is in RGB color space, we developed a technique to make use of all channel information by linearly combining the channels using weights $A_1, A_2, \text{and } A_3$.

For each pixel of the sample plate image, the normalized result is a dot product between chosen parameters (A_1, A_2, A_3) and (R, G, B) red, green, blue pixel intensity of the sample plate subjected to the constraint that:

$$A_1 R_{bg} + A_2 G_{bg} + A_3 B_{bg} = 1$$

where (R_{bg}, G_{bg}, B_{bg}) are red, green, blue intensity of the blank plate.

Assume that quantization noise Q dominates other noise sources and is a constant. Since error on R, G and B is Q, error on the normalized result is:

$$A_1^2(\Delta R)^2 + A_2^2(\Delta G)^2 + A_3^2(\Delta B)^2$$

$$= A_1^2 Q^2 + A_2^2 Q^2 + A_3^2 Q^2$$

$$= (A_1^2 + A_2^2 + A_3^2) Q^2$$

We need to pick (A_1, A_2, A_3) to minimize $(A_1^2 + A_2^2 + A_3^2)$.

Theorem 1:

$(A_1^2 + A_2^2 + A_3^2)$ is minimized when

$$A_1 = \frac{R_{bg}}{R_{bg}^2 + G_{bg}^2 + B_{bg}^2}$$

$$A_2 = \frac{G_{bg}}{R_{bg}^2 + G_{bg}^2 + B_{bg}^2}$$

$$A_3 = \frac{B_{bg}}{R_{bg}^2 + G_{bg}^2 + B_{bg}^2}$$

Proof:

By Cauchy–Schwarz inequality:

$$(A_1^2 + A_2^2 + A_3^2)\left(R_{bg}^2 + G_{bg}^2 + B_{bg}^2\right) \geq A_1 R_{bg} + A_2 G_{bg} + A_3 B_{bg} = 1$$

$$\leftrightarrow A_1^2 + A_2^2 + A_3^2 \geq \frac{1}{R_{bg}^2 + G_{bg}^2 + B_{bg}^2}$$

Equality happens at A_1, A_2, A_3 as stated.

The procedure to differentiate spots is described in Algorithm 3. Furthermore, from spot absorption measurements, we can predict the concentration of the unknown sample given concentrations of calibration samples using line fitting.

Algorithm 3: Spot differentiation

1. Normalize the intensity of each spot with the corresponding background part using formula in Theorem 1.
2. Integrate the absorption of the 441 intensity pixels around the center of each spot. At a specific pixel location, if the normalized intensity is **a**, absorption is then 1 – **a**.
3. Based on the absorption values, differentiate spots.

4.5 Multi-spot processing

Unfortunately, the single spot analysis steps cannot be applied directly to multi-spot analysis due to illumination constraint as shown in Fig. 5. We successfully detected the front line and the origin line as in Fig. 5(b). However, it is hard to pick up the spot in the middle of the right most column as in Fig. 5(c).

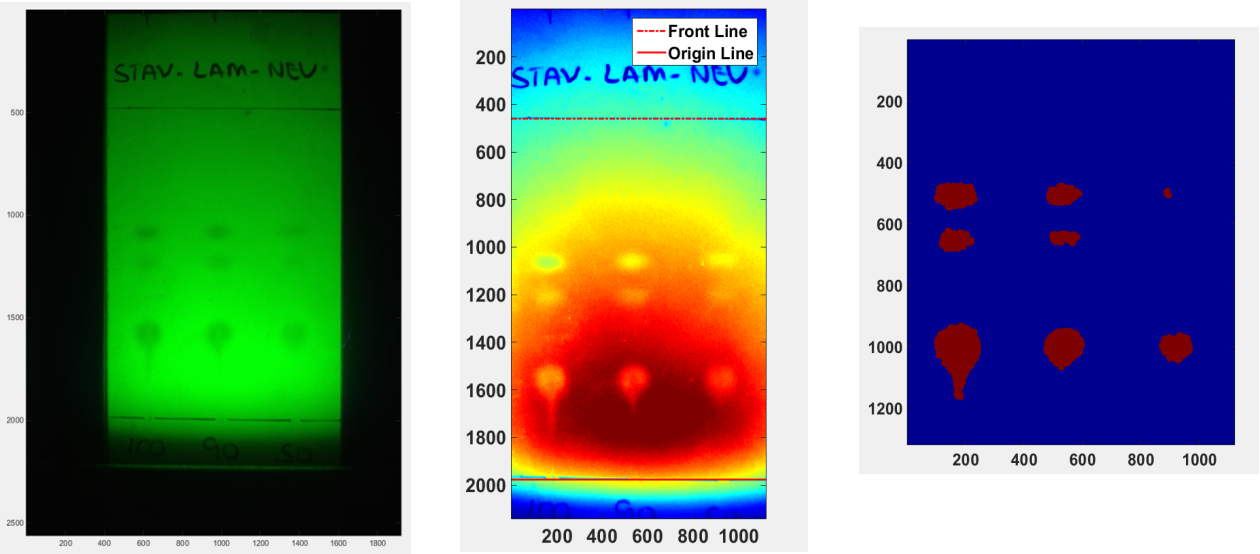

(a) (b) (c)

Figure 5: (a) Multi-spot sample image. (b) Result of line detection. (c) Result of spot detection.

5. Absorption-based biological assays

This section describes the hardware and software that we developed to demonstrate absorption-based biological assays by performing an enzyme-linked immunosorbent assay (ELISA) experiment. We start with the hardware design, then move on to software design which consists image processing steps that process captured ELISA images and user interface to guide unexperienced users through assay steps.

5.1 Hardware design

The hardware was designed and fabricated by Kenneth D. Long. A Samsung Galaxy S3 was used as the smartphone, and a 3D custom designed cradle was used as the spectrometer for the absorption measurements. This cradle was designed with several optical components in alignment to maximize the collection of transmitted light to the CMOS chip as shown in Fig. 6. The CMOS images captured by the smartphone show full spectra from 400nm to 700 nm, which accounts for most of the visible range. Figure 7(a) shows the spectral response through a cuvette of water, which we refer to as broadband image. Figure 7(b) shows the spectral response through yellow dye, so other colors are absorbed and the yellow appears as a mix of red and green. Figure 7(b) is referred to as a sample image.

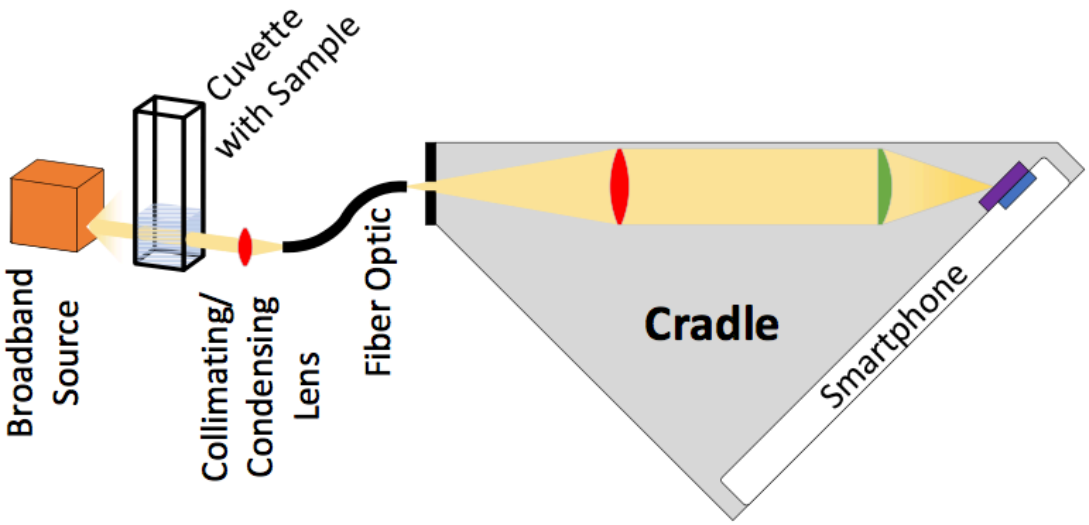

Figure 6: Absorption modularity cradle design (figure drawn by Kenneth. D. Long)

(a) (b)

Figure 7: (a) Broadband image. (b) Yellow dye sample image

5.2 Software design

The goal of the App is to enable an unskilled user to perform assays accurately and provide the user with assay results. The results can also be delivered to an online database and seen by a physician in order to perform more complex analysis. The App also enables the user to combine assay results and shows full spectral images. To achieve these goals, we provide a user interface that guides the user through the steps of performing an assay and completely hides the computation steps (image analysis, calibration. Etc.) from the user. We pop up messages when the user makes an error and ask them to redo that. The App is also capable of communicating securely with Dropbox, enabling a user to replicate all images and analysis in the cloud. The high-level diagram for performing the assay is in Fig. 8:

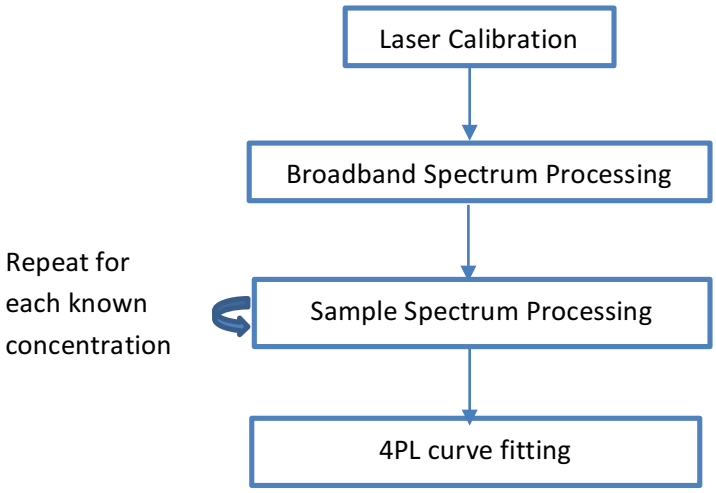

Figure 8: Assay performing procedure

Each step of the procedure then goes through a chain of image processing. The full image analysis pipeline is illustrated in Fig. 9 (not all the steps follow the complete chain of processing).

Figure 9: Image analysis pipeline

The analysis is computationally intensive and takes around 6.5 seconds on average on the phone. Therefore, to avoid putting a burden on the UI thread, we choose to process the analysis in the background using an asynchronous task that posts results back to the UI thread. This way of processing also allows us to render a progress dialog to notify the user to wait while we are processing.

5.2.1 Pre-processing

We use pre-processing algorithm in order to extract the color part in a typical ELISA image (Fig. 7), which is the signal we are interested in.

Algorithm 1: Extract the color part in a typical ELISA image

1. Sum pixel intensities in the horizontal direction.
2. Get the 70-percentile threshold.
3. Extract indexes with pixel intensities larger than the threshold.
4. From indexes got from step 3, extract its “continuous” part based on the criterion that the gap between two indexes is less than or equal to 100.
5. Check if we have at least 20% of data, otherwise raise an error.
6. Record the start and end of the interval to prepare for the next step.

5.2.2 Laser calibration

Since the spectrum moves around in the images produced by the camera due to motion of the cuvette in the cradle, we must calibrate the system by finding the position of a known wavelength. We then assume a linear relationship (measured once, in advance) between wavelength and position in the image. To find a known point, we use a green laser of wavelength 532 nm for calibration. The following algorithm shows how we process an image of a green laser illumination to get the corresponding pixel value.

Algorithm 2: Calibrate green laser

1. Pre-processing (see Algorithm 1 above)
2. Circle fitting:

   We will fit a circle through the interest interval of data extracted in the preprocessing step.

   For percentage p from -90 to 90 (except 0):

   a. For each column from start to end of the interval extracted in the preprocessing step, find point which is p% from the maximum pixel intensity.
   b. Points from step a may contain some outliers; we use the test of two standard deviations from the mean to remove outliers.
   c. Fit a circle through points and record the error as well as the intersection with the horizontal axis.

   Choose the circle which gives us the least mean square error.

3. Integration
   a. From the minimum and maximum intersection with the horizontal axis in the previous step, integrate along the circle.
   b. Based on the integrated spectrum results from step 3(a), fit a third degree polynomial to find the peak of laser.

5.2.3 Spectrum processing

We use the same algorithm to process broadband and sample spectra

Algorithm 3: Process a broadband spectrum or sample spectrum

1. Pre-processing (see Algorithm 1 above)
2. Circle fitting: Like the circle fitting step of laser calibration except that we do not record the intersection with horizontal axis since we will integrate entirely from 0 to width – 1 of the image (we use the same normalization technique to merge RGB channels as shown in Section 4.4).
3. Integration

Perform integration from 0 to width – 1 of the image along the circle found in step 2; we get a 1D spectrum.

4. Convert from pixel positions to wavelengths by linear mapping using the pixel value of green laser.
5. Measure absorption at 450 nm.

5.2.4 Absorption measurement

From 1D spectrum of broadband and sample measurement, we will be able to get the absorption by subtracting sample measurement from broadband measurement.

5.2.5 Four parameter logistic regression

Absorption measurements in ELISA assays can vary by many factors outside of the control of the experimenter, such as ambient temperature. Such assays generally make use of a set of known concentrations and curve-fitting in order to account for these unknowns. In particular, the absorptions for samples with known concentrations are fit to an S-curve using four parameter logistic regression (4PL) [11] to find the mapping between known concentrations and absorption values, which can then be measured as discussed in Section 5.2.4:

$$y = d + \frac{a - d}{1 + (\frac{x}{c})^b}$$

where

a = the minimum value that can be obtained

d = the maximum value that can be obtained

c = the point of inflection

b = Hill's slope of the curve

x = the known concentration value

y = the absorption measurement for the corresponding known concentration

6. Lessons learned and challenges

In this chapter, we generalize some of the lessons learned and challenges faced during development of the TLC and ELISA applications in order to provide a broader and more useful picture for developing smartphone bioassay applications in general.

6.1 Unstable and uneven illumination

To keep our TLC platform affordable in developing countries, we use an inexpensive ($50) UV lamp for illumination. However, this lamp's illumination is uneven and unstable, both of which lead to difficulty in processing the resulting images.

6.1.1 Unstable illumination

To show that the combination UV lamp illumination and TLC plate is unstable, we performed the following experiment:

- Put a TLC plate inside the cradle.
- Turn on the UV lamp and let the camera take 1024 consecutive images. The phone can take a photo roughly once per second.
- Divide and label a TLC image into multiple regions as shown in Fig. 10, each region having roughly 300 pixels.
- Average the intensity in each region of each image.

This experiment produces 1024 data points for each of the nine regions. The results appear in Fig. 11. Average intensity increases over time, asymptotically approaching a stable value. It takes around one second to take one photo. From Fig. 11, the average intensities reach the stable points around image 200. Thus, it takes us around 200 seconds to get a stable signal.

We did further analysis on region (1, 1) by taking each pixel in each region and subtracting its intensity from the average intensity of that region. This gives us the pixel error of each region. We plot the error of regions in Fig. 12. As shown in the figure, pixel error is skewed when the lamp is cold (the first 200 photos), but gradually converges to a classic Gaussian-like shape.

We also wondered whether the phosphorous material of a TLC needs time to reach a stable stage. To show that the problem came from the UV lamp itself, we did the following experiment:

- Warm up the UV lamp for 200 seconds.
- Put a TLC plate inside the cradle and let the camera take 1024 consecutive images.

- Divide and label a TLC image into multiple regions as shown in Fig. 10, each region having roughly 300 pixels.
- Average the intensity in each region of each image.

The key difference between the second experiment and the first is that the UV lamp is warmed up for 200 seconds prior to insertion of the TLC plate. If the variation arises from the lamp, we expect to see the same results as from the previous experiment, but shifted by 200 photos. If, however, variation is due to the plate, we expect to see results similar to those of the last experiment. The result of this experiment is shown in Fig. 13. There is no fluctuation in the signal of each region.

We also did the same analysis as above for region (1, 1) as shown in Fig. 14. There is no shift in the Gaussian shape.

To conclude this challenge, there is evidence that the UV illumination changes over time until it reaches some stable state. That time is 200 seconds for our UV lamp model. Therefore, we need to warm up the UV lamp for 200 seconds before doing an experiment. If the lamp is not warm enough when photos are taken, the illumination level of the blank plate photo (taken second) is higher on average than that of the TLC plate photo (taken first), leading to artificially high absorption estimates.

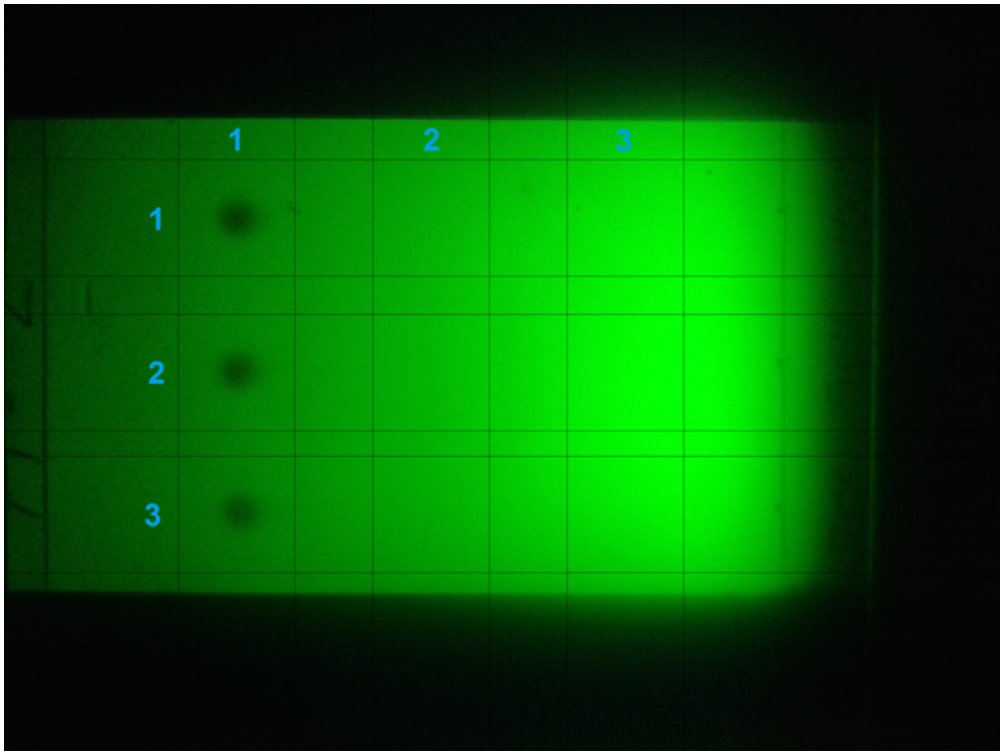

Figure 10: Region based division of a TLC image

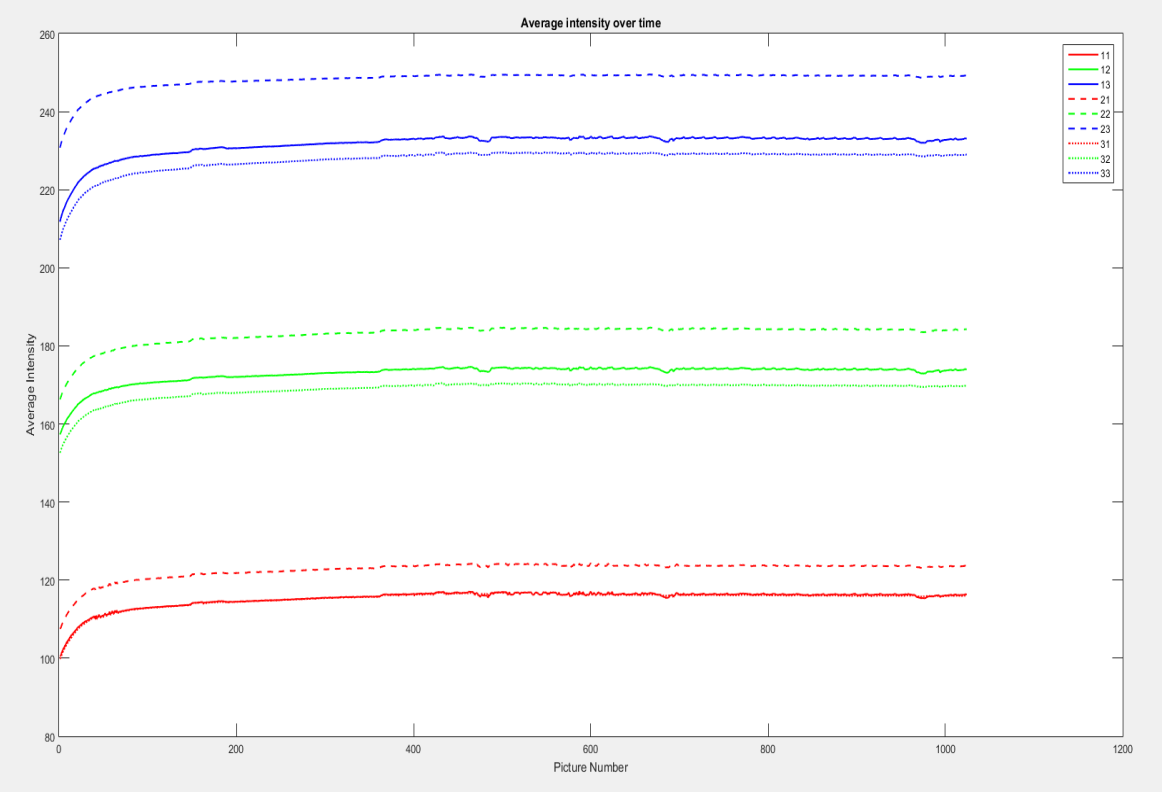

Figure 11: Average TLC image intensity for each region over time without warming up the UV lamp

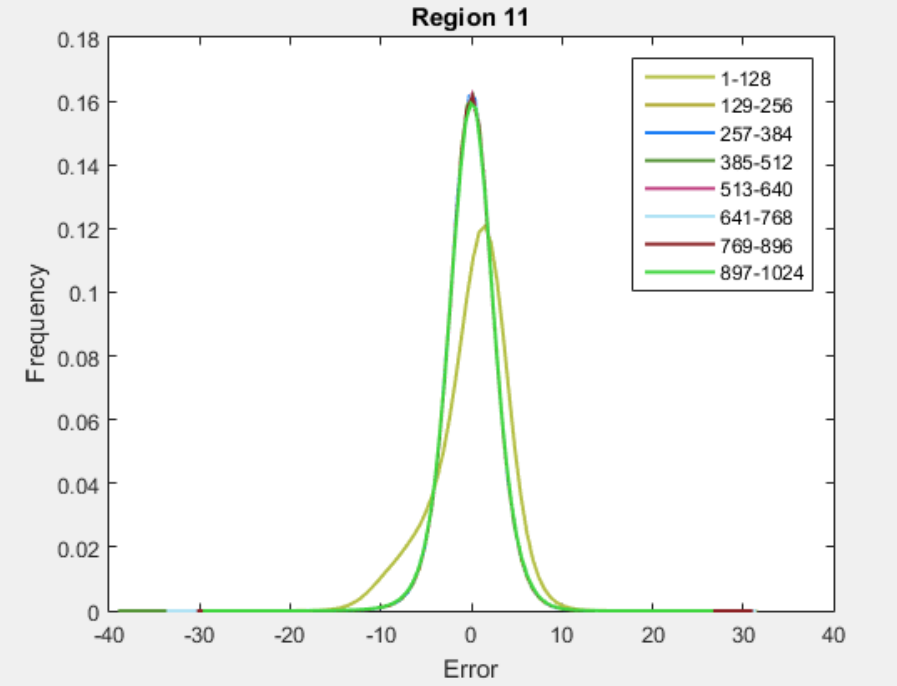

Figure 12: Error analysis of region (1, 1) without UV lamp warming up

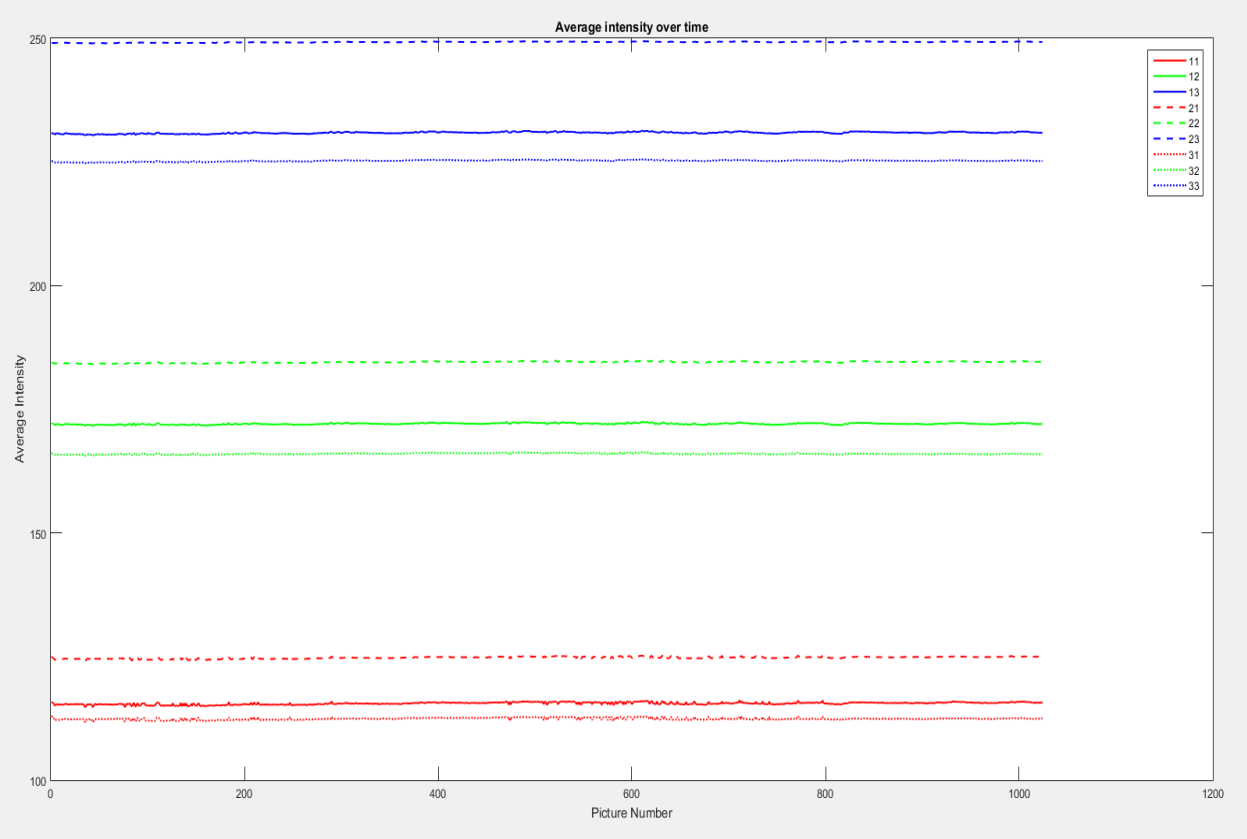

Figure 13: Average TLC image intensity for each region over time with warming up the UV lamp

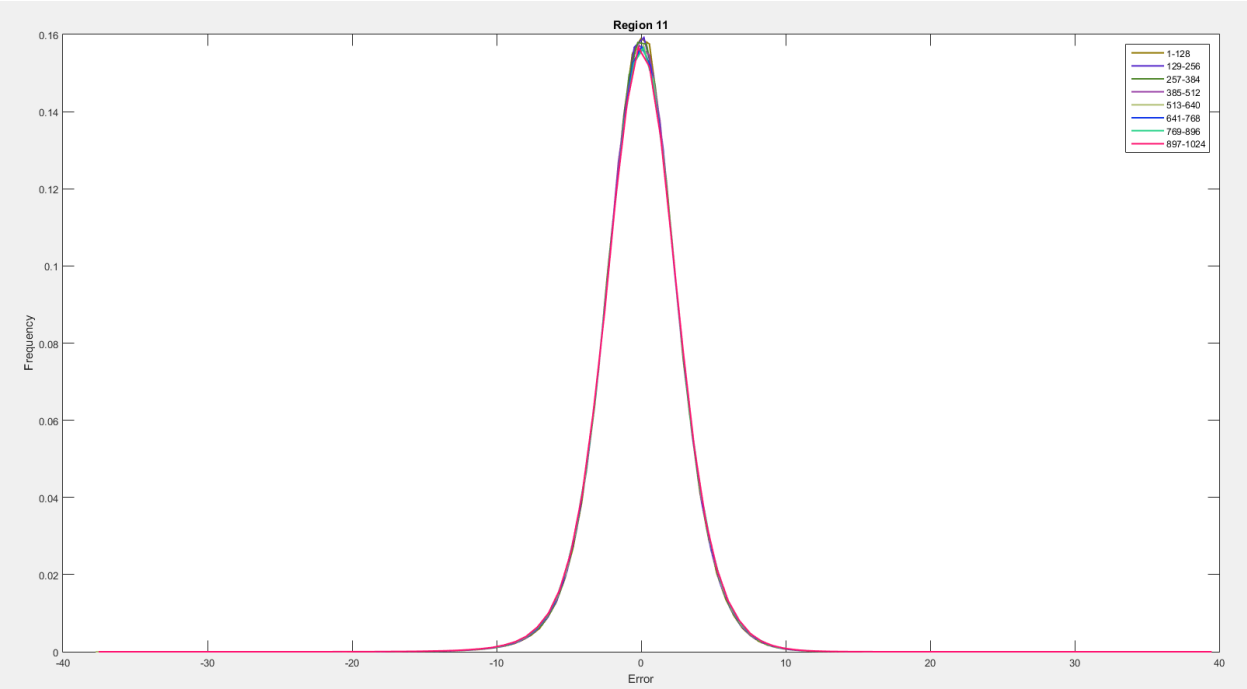

Figure 14: Error analysis of region (1, 1) with UV lamp warming up

6.1.2 Uneven illumination

As discussed previously, illumination is not uniform across the TLC plate. There is a region in the center of the image in which the camera's sensors are saturated (and thus artificially underreport the brightness), and the image fades off towards each edge. To solve this challenge, we introduced the idea of normalization by using a blank plate as pointed out in Section 4.3. In order to achieve consistent results, the two images must be at the same focus distance as well as having the same white balance compensation and exposure value. Since there is nothing to focus on the blank plate, we decide to call the autofocus procedure when we take the chromatoplate image and later keep that focus value for the blank plate. The problem with this approach is that the phosphorous material of the plate fades off over time and the intensities of the TLC sample plate and TLC blank plate may not match to each other.

6.2 Thin layer chromatography modeling

The model for thin layer chromatography is not well studied in the literature. Ryder suggests a model of infinite layers of a chromatoplate [12] but his mathematics does not apply directly to our system. In section 3.4.4, we suggested the ratio between the sample plate intensity and the blank plate is proportional to the concentration of the drug; we call this model the absorption model. However, Stern-Volmer [13] proposed that the ratio between the blank plate and the sample plate is proportional to the concentration of the drug. In summary,

- Absorption model:

$$\frac{sample}{blank} = 1 - k_1 * c$$

where k_1 is some constant and C is the concentration.

- Stern-Volmer model:

$$\frac{blank}{sample} = 1 + k_2 * c$$

where k_2 is some constant and C is the concentration.

The result is summarized in Table 3. The mean square error of the absorption model is 11.55 and the mean square error of the Stern-Volmer model is 11.2. Thus, the performances of the two models are roughly the same.

Table 3: Comparison of absorption model and Stern-Volmer model

				Absorption Model			Pred	S-V Model			Pred
A2	75	95	100	202.18	184.61	171.17	89.17	962.39	1054.95	1137.93	88.18
A3	75	95	100	211.88	203.02	190.77	85.49	920.01	958.44	1020.38	84.57
N1	75	95	100	287.76	269.17	253.69	88.64	676.19	722.87	767.49	87.78
N2	75	95	100	257.44	247.56	231.17	84.41	755.96	785.88	841.76	83.72
N3	75	95	100	277.55	260.82	247.22	88.80	701.10	746.08	787.10	88.08
P1	75	95	100	233.56	223.67	199.35	82.22	832.75	869.64	975.75	81.45
P2	75	95	100	253.93	241.95	232.39	88.91	766.25	804.27	837.47	88.35
P3	75	95	100	236.01	232.16	209.11	78.58	824.55	838.16	930.95	78.20
A2	100	50	75	223.83	287.91	262.62	58.70	869.77	676.08	741.06	62.38
A3	100	50	75	232.12	295.89	265.25	51.87	838.26	657.65	734.05	56.67
N1	100	50	75	264.65	327.39	289.71	37.42	735.60	594.19	671.89	44.52
N2	100	50	75	283.23	325.86	295.18	10.77	687.01	596.99	659.14	19.26
P2	100	50	75	232.59	272.11	247.56	33.97	836.66	714.85	786.28	39.56
P3	100	50	75	221.99	272.27	255.42	62.40	876.86	714.63	762.09	64.66
A2	100	90	75	262.79	276.04	280.30	81.09	740.44	705.28	694.32	80.94
A3	100	90	75	252.12	267.77	273.82	81.97	771.87	726.59	710.58	81.53
N2	100	90	75	244.33	249.19	255.70	89.30	796.30	780.69	760.92	88.97
N3	100	90	75	240.87	247.37	256.82	89.81	807.71	786.89	757.56	89.62
N3	100	90	75	274.54	289.29	312.08	90.18	708.76	672.51	623.37	89.39
P3	100	90	75	215.40	230.96	244.39	86.58	903.56	842.52	796.23	85.78
A1	100	90	80	222.11	239.64	248.94	86.93	876.26	811.91	782.32	86.30
A3	100	90	80	221.81	243.77	248.46	83.51	877.55	798.48	783.50	83.19
N1	100	90	80	243.05	252.62	255.41	84.52	800.64	770.16	761.83	84.29
N2	100	90	80	281.00	286.40	287.84	84.22	692.36	679.42	676.11	84.08
P1	100	90	80	176.41	192.59	199.24	85.83	1103.13	1010.64	976.88	85.35

6.3 Camera characteristics

Since the smartphone camera is designed to take images of our daily life and not images of biological experiments, there are a lot of unknown image processing algorithms that introduce noise to our data such as ISO (ADC gain), image compression and post image processing algorithm (e.g., white balance, etc.). Deducing the details of these algorithms and inverting their effect on photographs is quite challenging. In later projects, we were able to use raw camera sensor output (using Android Camera API 2), which sidesteps this question entirely. However, only expensive, state-of-the-art smartphones currently offer this option.

One effect that we were able to measure and address is the variation in individual pixels from photo to photo. The source of these variations may be the plate itself, or the camera sensors, or the unknown image processing algorithms being executed on our behalf.

We measured and plotted pixel noise in Fig. 15, which exhibits a Gaussian-like shape, so we believe that noise is random. In that case, image averaging would work well.

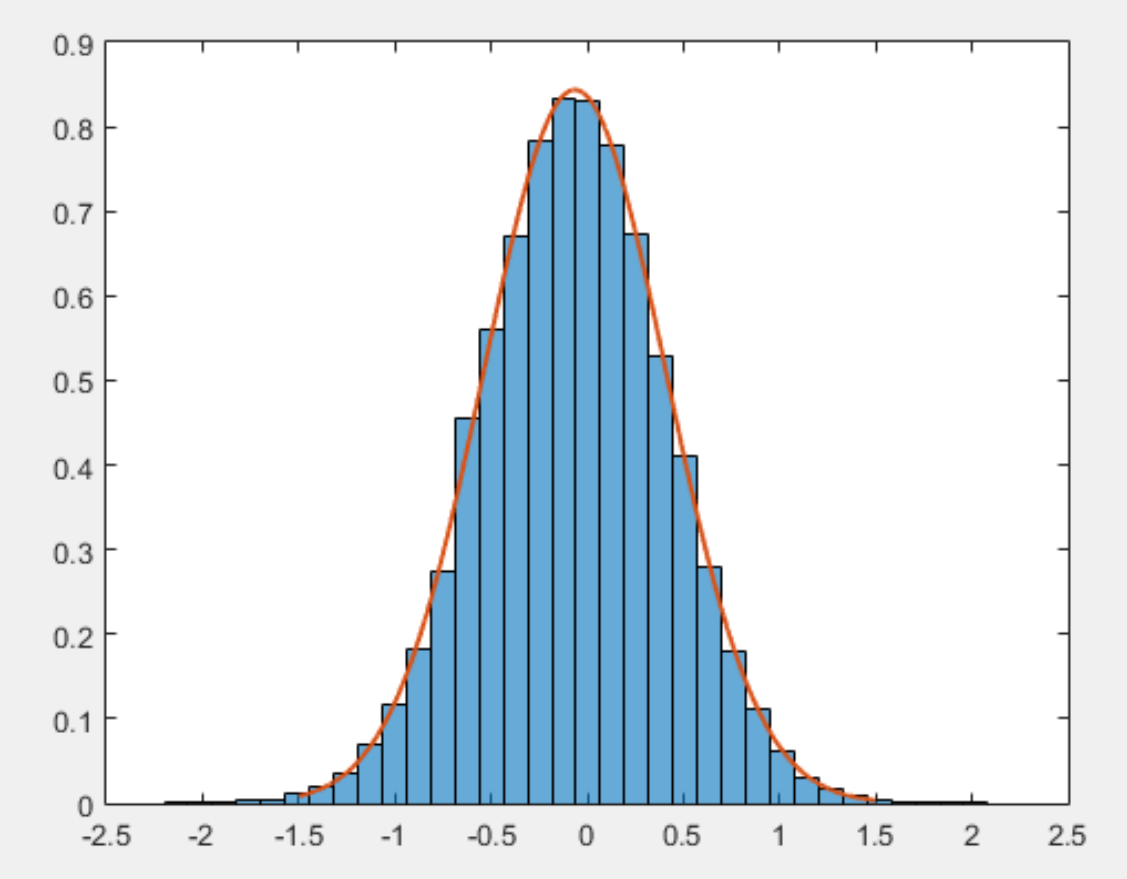

Figure 15: Pixel noise of TLC image

Also, it is worth mentioning that some camera settings produce better results than others. For TLC application, we found that daylight white balance and ISO of 200 works best. For ELISA application, we found that incandescent white balance and ISO of 100 works best.

6.4 Optimization for smartphone computation

6.4.1 Optimization using single instruction multiple data (SIMD) instructions

Our original implementation of TLC analysis was fairly slow for the user. To understand the problem, we measured and broke down the timing of TLC processing:

- Reading an image using libjpeg takes about 500 milliseconds
    - 10 blank images: 500 milliseconds * 10 = 5 seconds
    - 10 sample images: 500 milliseconds * 10 = 5 seconds

  In total, reading images takes about 10 seconds.
- Image averaging: 25 seconds per set. In total, averaging images takes about 50 seconds.
- Additional image processing: 20 seconds total.

In total, TLC analysis required 80 seconds, and image averaging is clearly the bottleneck, taking 62.5% of the total time.

The ARM v9 CPU in the Samsung Fame 6810 supports Neon single instruction multiple data (SIMD) instructions to accelerate multimedia and image processing algorithms, so we rewrote the image averaging part using Neon instructions. As shown in Table 4, this change reduces the processing time significantly, from 25 seconds per set down to 4 seconds per set. Total time for TLC analysis reduces to 38 seconds, less than half of the original time.

Table 4: Timing measurement for image averaging with and without Neon optimization

Image averaging without Neon	Image averaging with Neon
25 seconds	4 seconds

6.4.2 Filter consideration

Image filtering plays an important role in our image processing algorithms. For example, we used Gaussian filter as a low-pass filter to denoise when detecting lines in Section 4.2. To have fast image denoising with large filter, we need to choose large filters that can be decomposed into multiple smaller filters. For TLC, we chose Gaussian filter since 2D Gaussian filter is a separable filter, it can be decomposed into two 1D filters: one horizontal and one vertical.

6.5 Hardware design

Originally, the TLC cradle was fabricated from white plastic, as shown in Fig. 2. The final design uses opaque, black plastic as shown in Fig. 16. The reason for the change is that the white cradle version lets the environmental light pass through and affect the TLC image we capture. This effect is demonstrated

in Fig. 17, which shows sample TLC images taken using the white cradle with and without environmental lighting. Such lighting adds unnecessary noise to the TLC image. We discovered this drawback in the original (white) design by comparing TLC images taken in a bright environment with images taken in a dark environment. The difference in pixel intensity between such images is about 20 on average (about 8% of the full scale of an 8-bit-per-channel image).

Figure 16: Final cradle version.

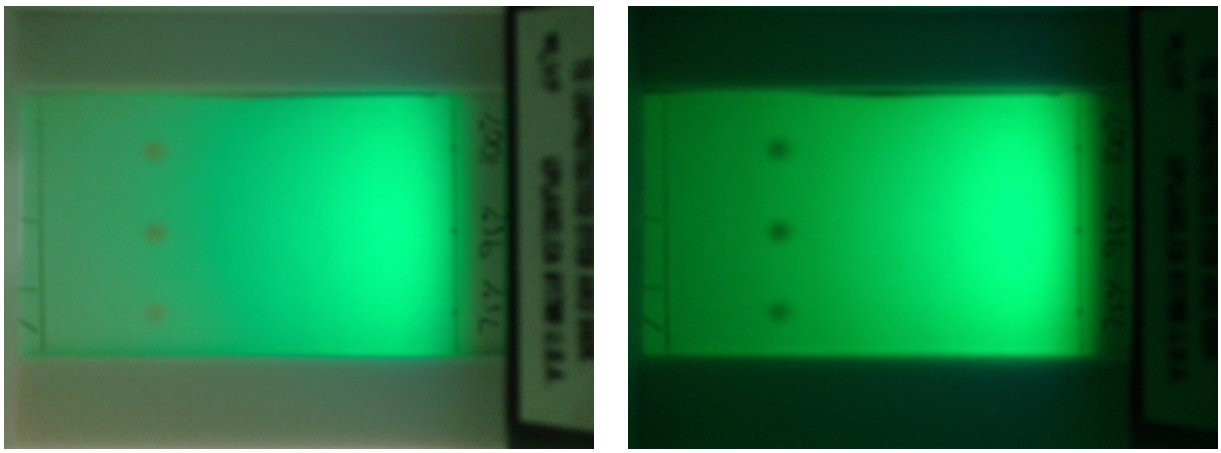

(a) (b)

Figure 17: (a) Sample TLC image with environment lighting. (b) Sample TLC image without environment lighting.

7. Conclusion

In this work, we demonstrate two working applications to perform biological experiments on a smartphone. The hardware was fabricated using a 3D printer and the software was written to run on Android smartphones. The algorithms we developed are efficient to run on a computationally limited platform like a smartphone. We described challenges, such as unstable and uneven illumination, thin layer chromatography modeling, the noise introduced by unknown image processing algorithms, hardware design, filter consideration and discussed how we overcome those challenges. We also presented how we optimized the smartphone computation using Neon SIMD instructions to reduce a TLC analysis time by more than half of the original time. Although we have successfully solved two problems in this space, generalizing the approach remains incomplete. There are still many problems that remain to be solved, as smartphone cameras are not designed for biological experiments.

References

[1] World Health Organization Web site. http://www.who.int/medicines/services/counterfeit/impact/TheNewEstimatesCounterfeit.pdf

[2] AfricaRenewal Web site. http://www.un.org/africarenewal/magazine/may-2013/counterfeit-drugs-raise-africa%E2%80%99s-temperature (accessed 12.06.2016)

[3] H. Yu, H. M. Le, E. Kaale, K. D. Long, K. D. Layloff , S. S. Lumetta, B. T. Cunningham, Characterization of drug authenticity using thin-layer chromatography imaging with a mobile phone. Journal of Pharmaceutical and Biomedical Analysis, 125 (2016) 85-93

[4] D. Gallegos, K.D. Long, H. Yu, P.P. Clark, Y.X. Lin, S. George, P. Nath, B.T. Cunningham, Label-free biodetection using a smartphone, Lab Chip 13 (2013) 2124–2132.

[5] W. Zhang, A. Jones, M. Doherty, Does paracetamol (acetaminophen) reduce the pain of osteoarthritis?: a meta-analysis of randomised controlled trials, Ann. Rheum. Dis. 63 (2004) 901–907.

[6] A. Violari, J.C. Lindsey, M.D. Hughes, H.A. Mujuru, L. Barlow-Mosha, P. Kamthunzi, B.H. Chi, M.F. Cotton, H. Moultrie, S. Khadse, W. Schimana, R. Bobat, L. Purdue, S.H. Eshleman, E.J. Abrams, L. Millar, E. Petzold, L.M. Mofenson, P. Jean-Philippe, P. Palumbo, Nevirapine versus ritonavir-boosted lopinavir for HIV-Infected children, New Engl. J. Med. 366 (2012) 2380–2389.

[7] S.B. Sirima, A. Gansane, Artesunate-amodiaquine for the treatment of uncomplicated malaria, Expert Opin. Inv. Drug. 16 (2007) 1079–1085.

[8] World Health Organization Web site. http://www.who.int/selection_medicines/committees/expert/20/EML_2015_FINAL_amended_AUG2015.pdf (accessed 12.06.2016).

[9] R.C. Gonzalez, R.E. Woods, Digital Image Processing, third edition, Prentice Hall, New Jersey, 2008, pp. 657–761.

[10] The university of Edinburgh School of informatics Web site. http://homepages.inf.ed.ac.uk/rbf/HIPR2/open.htm (accessed 12.06.2016)

[11] MyAssay Web site. https://www.myassays.com/four-parameter-logistic-regression.html (accessed 12.06.2016)

[12] D. J. Ryder, Handbook of thin-layer chromatography (Chromatographic Sciences Series/55). Edited by: Joseph Sherma and Bernard Fried. Published: Marcel Dekker Inc., New York 1991, 1064pp.

[13] M. A. R. B. Castanho, M. J. E. Prieto, Fluorescence quenching data interpretation in biological systems: The use of microscopic models for data analysis and interpretation of complex systems, Biochimica et Biophysica Acta (BBA) - Biomembranes, Volume 1373, Issue 1, 14 August 1998, Pages 1-16.